Fuel 335 (2023) 127076

Contents lists available at ScienceDirect

Fuel

journal homepage: www.elsevier.com/locate/fuel

Thermal degradation characteristics, kinetic and thermodynamic analyses of date palm surface fibers at different heating rates

Abrar Inayat [a,b,*], Farrukh Jamil [c], Shams Forruque Ahmed [d], Muhammad Ayoub [e], Peer Mohamed Abdul [f], Muhammad Aslam [c], M. Mofijur [g,i], Zakir Khan [c,j], Ahmad Mustafa [h]

[a] Department of Sustainable and Renewable Energy Engineering, University of Sharjah, 27272 Sharjah, United Arab Emirates
[b] Biomass & Bioenergy Research Group, Center for Sustainable Energy and Power Systems Research, Research Institute of Sciences and Engineering, University of Sharjah, 27272 Sharjah, United Arab Emirates
[c] Department of Chemical Engineering, COMSATS University Islamabad, Lahore Campus, Lahore, Punjab 54000, Pakistan
[d] Science and Math Program, Asian University for Women, Chattogram, Bangladesh
[e] Department of Chemical Engineering, Universiti Teknologi PETRONAS, 32610 Perak, Malaysia
[f] Department of Chemical and Process Engineering, Faculty of Engineering and Built Environment, Universiti Kebangsaan Malaysia, 43600 Bangi, Selangor, Malaysia
[g] Centre for Technology in Water and Wastewater, School of Civil and Environmental Engineering, University of Technology Sydney, Ultimo, NSW 2007, Australia
[h] General Systems Engineering, Faculty of Engineering, October University for Modern Sciences and Arts (MSA), 12566, Egypt
[i] Mechanical Engineering Department, Prince Mohammad Bin Fahd University, Al Khobar, 31952, Saudi Arabia
[j] Biomass Conversion Research Centre, Department of Chemical Engineering, COMSATS University Islamabad, Lahore Campus, Lahore, Punjab 54000, Pakistan

ARTICLE INFO

Keywords:
Date palm waste
Pyrolysis
Kinetic analyses
Bio-oil
Waste management
Waste utilization
Coats–Redfern method

ABSTRACT

The potential of the least-exploited date pam waste was presented as feedstock for bio-oil production. The surface fibers of the date palm are widely available as waste material in the Gulf region, the Middle East, and Africa. Chemical composition analysis and physiochemical characterization showed that surface fibers are valuable feedstock for energy production. Surface fibers were analyzed thermogravimetrically at different heating rates (10, 20, and 30 °C /min) in an inert atmosphere. Decomposition was carried out in three stages: dehydration, devolatilization, and solid combustion. Kinetic analysis was performed on the devolatilization region using the Coats–Redfern model–fitting method using twenty–one reaction mechanisms from four different solid-state reaction mechanisms. Two diffusion models: one–way transport ($g(x) = \alpha^2$) and Valensi equation ($g(x) = \alpha+(1-\alpha) \times \ln(1-\alpha)$) showed the highest regression coefficient (R^2) with the experimental data. The activation energy (E_a) and the pre-exponential factor (A) was estimated to be 91.40 kJ/mol and 1.59×10^3 –29.39×10^3 min^{-1}, respectively. The kinetic parameters were found to be dependent on the heating rate. The surface fibers' thermodynamic parameters ΔH, ΔG, and ΔS were 80–97, 151–164, and −0.17- −0.18 kJ/mol, respectively. This indicates that the pyrolysis of surface fibers is endothermal and not spontaneous. Since there is not much experimental work on the pyrolysis of surface fibers available in the literature, the reported results are crucial for designing the pyrolysis process.

1. Introduction

In recent years, the global demand for sustainable and renewable energy has increased due to uncertain fossil fuel supply, rapid industrial growth, increasing population, and stringent environmental regulations [1,2]. Currently, nearly 80 % of the world's primary energy consumption comes from oil, natural gas, and coal [3]. The transport sector consumed about 29 % of total energy in 2015, with 96 % of fuels coming from petroleum [4]. In 2017, about 97.50 million barrels of liquid fuel per day were expected to be consumed [5]. At the same time, transportation-related CO_2 emissions amounted to 7 billion metric tons, accounting for a quarter of global CO_2 emissions. As a result, the ever-increasing demand for petroleum fuels and the environmental problems associated with their use have led experts to look at renewable energy sources [6]. In this context, organic waste, especially lignocellulosic waste materials, has a promising future [7,8]. Lignocellulosic waste is an abundant and long-term renewable energy source. Biomass generation at the global level is estimated to exceed 220 million tons per

* Corresponding author at: Department of Sustainable and Renewable Energy Engineering, University of Sharjah, 27272 Sharjah, United Arab Emirates.
E-mail address: ainayat@sharjah.ac.ae (A. Inayat).

https://doi.org/10.1016/j.fuel.2022.127076
Received 18 October 2022; Received in revised form 15 November 2022; Accepted 4 December 2022
Available online 13 December 2022

Fig. 1. Date palm surface fibers.

year [9]. For example, the United Arab Emirates has nearly 40 million date trees, with Abu Dhabi accounting for 75 percent of the total. Each tree produces about 15 kg of biomass waste yearly, including dried leaves, rachis, fronds, date seeds, fibers, and other materials. Each year, nearly 2 million tons of palm dates are produced and wasted during production[10].

Gaseous, liquid, and solid fuels can be produced from biomass waste using a variety of processes. Pyrolysis is a thermochemical conversion process that produces bio-oil, biochar, and pyrolytic gasses from various biomasses [11]. Pyrolysis is the thermal degradation of material in an inert atmosphere. The three main categories are slow, fast, and flash pyrolysis, which is ascertained by the temperature range, heating rate, and residence time. Fast pyrolysis produces bio-oil, also known as pyrolysis oil. Fast pyrolysis has a moderate temperature (300–700 °C), a faster heating rate of 10–200 °C/min, and a quick solids retention time of 0.5–10 s [12]. Bio-oil synthesis from fast pyrolysis of lignocellulosic waste materials is a promising candidate for replacing conventional fuels because it is clean and renewable. Its combustion produces very low levels of SO_x and NO_x emissions [13,14]. Bio-oil has the potential to be used in boilers, turbines, and vehicle engines, as well as to produce a variety of high-value compounds [15]. The bio-oil yield depends on the amount and type of volatiles extracted from a feedstock [16]. Biochar, the main by-product of slow pyrolysis, can be produced from lignocellulosic wastes. Because biochar contains a very stable carbon component, it was initially proposed as a soil amendment to sequester carbon in the soil [17]. It can be used as a soil amendment to improve soil health, as a nutrient and microbial carrier, as an immobilizing agent to remove toxic metals and pollutants from water and soil, as a catalyst for industrial purposes, as a porous medium to reduce emissions of greenhouse gases and odorous substances, and as a supplemental feed to improve the health and productivity of wildlife through more effective nutrient uptake [18]. Pyrolysis is the only thermochemical conversion process producing products in all three forms (solid, liquid, and gas). Gasification is also a thermochemical process that produces syngas (CO + H_2) under partial oxygen conditions. Synthesis gas can be used for power generation. However, unlike other thermal conversion processes, the products of pyrolysis are suitable for storage and transportation [19].

Lignocellulosic biomasses consist of cellulose, hemicellulose, and lignin in varying proportions. Cellulose is mainly responsible for bio-oil production [20,21]. In thermogravimetric analysis, a technique for pyrolysis of solid materials, the decomposition of lignocellulosic biomasses occurred in three regions [22]. The devolatilization region or active pyrolysis zone is the pyrolysis section where cellulose, hemicellulose, and little lignin decompose. The volatiles from this pyrolysis zone escape and a significant mass loss occurs in this region. The volatiles from the active pyrolysis zone is then condensed to form bio-oil [23]. The residue after the active pyrolysis zone is the carbon-rich material called biochar [24]. Biochar can be used in various fields, such as soil fertilizer, catalyst, energy production, composite materials, and many other purposes [25]. Kiman Silas et al. [26] review the applications of biochar and conclude that it can produce cost-effective catalysts to overcome the limitations of conventional catalysts such as short catalyst life, additional pollutant production, high capital cost, and temperature limitations. Safa Gamal et al. [27] prepared charcoal-based activated carbon as a catalyst from waste coconut shell for the deoxygenation of palm fatty acid distillate. Junaid Ahmed et al. [28] prepared solid-acid catalyst from biochar for biodiesel production. Ninety-six percent of the ester was reacted with a solid acidic charcoal-based catalyst. The catalyst had excellent catalytic activity, yielding 70 % conversion after five uses. Therefore, identifying and understanding the kinetics of the active pyrolysis region before performing pyrolysis is very important. This helps in a detailed understanding of the mechanism, performing selective pyrolysis, designing pyrolyzers, and performing pyrolysis under predetermined optimal conditions.

Each date palm produces a variety of waste materials, including leaves, vapors, stem wood, rachis, surface fibers, and seeds. The typical annual production of a date palm includes 20 kg of dry leaves, and date seeds account for 10–12 % of the date fruit [29]. Surface fibers of the date palm are lignocellulosic materials that are abundant as municipal and agricultural wastes in the United Arab Emirates and the Gulf region [30]. Surface fibers have yet to be examined at various heating rates to predict their kinetics and comprehend the pyrolysis behavior. To understand the reaction mechanism of pyrolysis and predict more accurate activation energy values, one needs to understand the effects of the heating rate. In addition, the estimation of the kinetic parameters at various heating rates helps to understand the accuracy of the model reaction mechanism. Moreover, to the best of the author's knowledge, no experimental work on the pyrolysis of date palm surface fibers has been published. Therefore, it is valuable to highlight the valorization of unattended waste materials.

Therefore, this is the first study to present a thermogravimetric analysis of date palm surface fibers at various heating rates (10, 20, 30 °C /min). Coats-Redfern model fitting evaluated the kinetic and thermodynamic parameters at different heating rates. The advantage of the Coats–Redfern method over model–free methods is that kinetic and thermodynamic parameters can be obtained at a single heating rate, and then the effects of the heating rate on these parameters can be observed. Other authors like Raza et al. [31] estimated the pyrolytic kinetic parameters of date palm waste using the Coats-Redfern integral method using different reaction mechanisms from the reaction, diffusion, geometric, and nucleation models. They found that the diffusion reaction mechanisms were the best-fit models. E_a in the main active pyrolysis region was 96–98 kJ/mol. Hani H. Sait et al. [31] estimated the pyrolytic and combustion kinetics of different date palm wastes using Coats-Redfern integral method. However, they only used a single reaction mechanism model. E_a in the main pyrolysis region varied from 32 to 43 kJ/mol. Galiwango Emmanuel et al. [32] estimated the pyrolytic kinetics of different date palm waste using the model-free method. They used Flynn–Wall–Ozawa (FWO), Kissinger–Akahila–Sunose (KAS), and Starink methods. The results were promising to declare the waste as a potential source for biorefinery. Moreover, no study has evaluated the effect of heating rate on the pyrolytic kinetics of date palm wastes. In this research work, the potential of date palm tree surface fibers as a renewable material for bio-oil or biochar production and their thermal

Table 1
Physiochemical properties of date palm fibers.

Analysis	Method	Properties
Proximate analysis	ASTM method	Volatile matter, fixed carbon, moisture, and ash content
Ultimate analysis	ASTM method using CHNS/O analyzer	Carbon, hydrogen, nitrogen, sulphur, and oxygen
Higher heating value (HHV)	Bomb calorimeter	HHV in MJ/Kg
Chemical composition analyses	TAPPI–T 204 cm-97	Extractables, pectins, waxes, etc.
	ASTM D1104-56	Lignin content
	ASTM D1103-60	α-cellulose content
	Holocellulose–α-cellulose	Hemicellulose
Density	(Obernberger and Thek, 2004)	Density in Kg/m^3
Functional chemistry analysis	IRTracer-100 FTIR spectrometer (Shimadzu, Kyoto, Japan) −(ATR-FTIR) with a range of 500 to 4000 cm^{-1}, an average of 34 scans, and a spectral resolution of 4 cm^{-1}.	Study the changes in functional groups at different wavelengths.

Table 2
Reaction mechanisms g(x) used in Coasts–Redfern model-fitting approach.

Mechanism	g(α)	Code
Chemical reaction		
0th order	α	CRO0
1st order	-ln(1-α)	CRO1
One and half order	2 [$(1-\alpha)^{-1.5}$-1]	CRO1.5
2nd order	[1/(1-α)]-1	CRO2
3rd order	0.5[$(1-\alpha)^{-2}$-1]	CRO3
Diffusion		
1-D transport	α^2	DM1
2-D transport	(1-α)-ln(1-α) + α	DM2
3-D transport	$[[-\ln(1-\alpha)]^{1/3}]^2$	DM3
Valensi equation	α+(1-α) ln(1-α)	DM4
Ginstling–Brounshtein equation	$(1-2\alpha/3)$ -$(1-\alpha)^{2/3}$	DM5
Zhuravlev equation	$[(1-\alpha)^{-1/3}$-1$]^2$	DM6
Jander equation	$[1-(1-\alpha)^{1/3}]^2$	DM7
Ginstling equation	1-(0.67α) -$(1-\alpha)^{0.67}$	DM8
Geometric		
cylindrical symmetry	$1-(1-\alpha)^{1/2}$	GM1
sphere symmetry	$1-(1-\alpha)^{1/3}$	GM2
Random nucleation and nuclei growth		
Power law(*P2*)	$\alpha^{1/2}$	NM1
Power law(*P3*)	$\alpha^{1/3}$	NM2
Power law(*P4*)	$\alpha^{1/4}$	NM3
Avrami-Erofeev equ. (when n = 2)	$[-\ln(1-\alpha)]^{1/2}$	NM4
Avrami-Erofeev equ. (when n = 3)	$[-\ln(1-\alpha)]^{1/3}$	NM5
Avrami-Erofeev equ. (when n = 3/2)	$[-\ln(1-\alpha)]^{2/3}$	NM6

degradation mechanism are presented along with kinetic and thermodynamic parameters at various heating rates that will help in carrying out their pyrolysis under predetermined optimal conditions.

2. Materials and methods

2.1. Materials

Surface fibers of the date palm tree were taken from a local farm in UAE as shown in Fig. 1. The fibers were rinsed with tap water and then placed in a convection oven at 105 °C for 48 h [33]. The fibers were then reduced to micrometer size using laboratory shredders. Laboratory crushers were used to reduce particle size and then sieved with 120 μm sieve plate.

2.2. Physicochemical characterization

Table 1 presents the summary of the analysis performed to evaluate physiochemical properties.

2.3. Thermal analysis

Thermal degradation of the fibers was determined by thermogravimetric analysis. A thermogravimetric analyzer (TGA Q 500 series, TA Instruments, USA) was used to analyze samples of 5–10 mg from a date palm at various heating rates 10–30 °C /min, and the mass loss of fibers from 20 to 800 °C. At a 60 ml/min rate, N_2 was used to keep the environment inert. The TGA of each respective heating rate was performed three times to obtain the lowest error and highest accuracy.

2.4. Kinetic parameters

The activation energy (E_a) and pre-exponential factor (A) was calculated by the Coats–Redfern approach. Coats–Redfern is a model-fitting method that helps in finding the kinetic parameters using the following equation (1) [34].

$$\ln\left[\frac{g(\alpha)}{T^2}\right] = \ln\left[\frac{AR}{\beta E_a}\right]\left(1-\frac{2RT}{E_a}\right) - \frac{E_a}{RT} \quad (1)$$

whereas,

g(α) represents different solid-state reaction mechanisms–21 reaction mechanism used in this study.

β is the rate of heating in °C/min–10, 20, 30 °C/min in this study.

R represents a gas constant–its value is taken as 8.321 × 10^{-3} kJ/mol.

T is the process temperature. It is taken on a kelvin scale (K).

A represents frequency factor or known as a pre-exponential factor–it is taken in.m^{-1}

α is the degree of decomposition–it is determined with equation (2)

$$\alpha = \frac{m_o - m_i}{m_o - m_f} \quad (2)$$

here, m_o is the initial mass of the date palm surface fibers sample when t = 0, m_i represents instantaneous mass, and m_f represents final mass of the sample.

A kinetic analysis can be performed using the Arrhenius equation, which defines the temperature dependence of the reaction rate. Equation (3) contains the formula of the Arrhenius law.

$$k(T) = A \times \exp\left(-\frac{Ea}{R \times T}\right) \quad (3)$$

The two required unknows: (I) activation energy (E_a) and (II) pre-exponential factor (A) can be found with equation (1). By plotting the L.H.S $\left(ln\left[\frac{g(\alpha)}{T^2}\right]\right)$ versus R.H.S $(1/T(K))$ of an equation (1). The slope of the straight line will be equal to $-E_a$/R, the value of E_a can simply be found by multiplying the slope's value with −8.321 × 10^{-3} kJ/mol. The intercept of this straight line will be equal to $ln\left[\frac{AR}{\beta E_a}\right]\left(1-\frac{2RT}{E_a}\right)$. The twenty–one solid-state reaction mechanisms used to define g(x) are presented in Table 2.

2.5. Thermodynamic parameters

The thermodynamic parameters (ΔH, ΔG, and ΔS) were derived using the kinetic parameters. Equations (4)–(6) represent the relations used to find the thermodynamic properties [35]:

Change in enthalpy

$$\Delta H = E_a - R \times T \quad (4)$$

Gibbs free energy

Table 3
Chemical composition of some lignocellulosic biomass materials.

Feedstock	extractives	cellulose	hemicellulose	lignin	Ref.
Date palm fibers	2.25 ± 5	43.10 ± 5	29.30 ± 5	25.35 ± 5	Current study
Oil palm bunch	–	59.14	12.07	25.33	[37]
Rice husk	–	35	33	23	[38]
Walnut shell	1.57	27.40	31.30	36.31	[39]
Olive waste	–	39.40	24.20	14.0	[40]
Date seeds	–	21.6	28.1	23.7	[41]
Date fronds	7.72	31.40	20.92	25.20	[42]

Table 4
Proximate and ultimate analysis of surface fibers.

Proximate analysis (percentage weight dry basis)	
Fixed carbon	10.20
Volatile matter	86.70
Ash	3.10
Moisture	3.50
Ultimate analysis (percentage weight dry basis)	
Carbon (C)	39.50
Hydrogen (H)	5.90
Nitrogen (N)	2.60
Sulphur (S)	0.65
Oxygen (O)*	51.35
Higher heating value (HHV) (MJ/kg)	17.25

*Calculated based on difference between 100 and sum of C, H, N, and S.

Table 5
Bulk density of various biomass wastes.

Biomass	Bulk density (kg/m^3)	References
Surface fibers (date palm)	405 ± 5	Current study
Date fruit seeds	450	[51]
Date leaf stem	216	[52]
Corn stover	160	[53]

$$\Delta G = E_a + R \times T_m \times ln\left(\frac{K_b \times T}{hA}\right) \quad (5)$$

Entropy

$$\Delta S = \frac{\Delta H - \Delta G}{T_m} \quad (6)$$

3. Results and discussion

3.1. Physiochemical characterization of surface fibers

Table 3 shows the chemical composition analysis of the surface fibers. It consists of 43.10 wt% cellulose, 29.30 wt% hemicellulose, and 25.35 wt% lignin. The information on the proportion of these three biopolymers is essential for performing selective pyrolysis and predicting the expected fuel yield. Cellulose can produce more bio-oil with a higher organic content, lower water content, and lower solids content. Hemicellulose produces a higher gas yield and moderate bio-oil with higher water content and lowers organic content. Lignin produces moderate bio-oil, lower gas yield, and significantly higher solids yield [36]. Therefore, lignocellulosic biomasses with higher cellulose content are preferred for bio-oil production, and biomasses with higher lignin content are preferred for biochar production. Table 3 relates the biopolymer composition of date palm tree surface fibers to that of other biomasses. Thus, this lignocellulosic waste has similar potential for use in the pyrolysis process.

Table 4 shows the proximity and ultimate analysis of surface fibers. The determination of the proximate and ultimate analysis, along with the higher heating value, means that the thermal properties were understood. Information on the amount of fixed carbon, volatiles, moisture content, and ash provides useful information on the behavior of the fuels during thermal conversion [43,44]. Surface fibers have a higher heating value (HHV) of 17.25 MJ/kg. The fibers have lower moisture and ash content, making them suitable for thermal conversion [45]. The higher volatile content of the fibers (86.70 wt%) makes them suitable for bio-oil production by pyrolysis [46]. Date fibers had total carbon (39.50 wt%), hydrogen (5.90 wt%), and a very small amount of nitrogen (2.60 wt%) and sulfur (0.65 wt%). The higher oxygen content (51.35 wt%) in the date fibers is responsible for forming undesirable oxygenated compounds during pyrolysis. The ultimate and proximate analysis results are comparable to other lignocellulosic materials [33,47–49].

The bulk density of surface fibers is shown in Table 5. Bulk density is an essential characteristic of biomass materials because it is related to

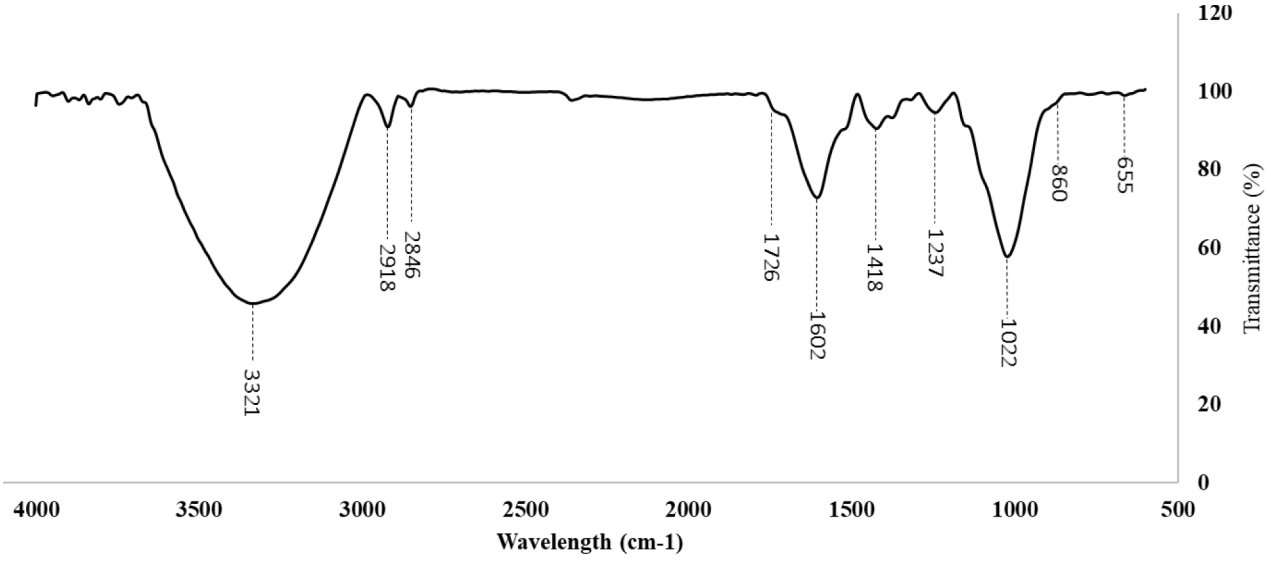

Fig. 2. FT–IR spectrum for surface fibers of date palm.

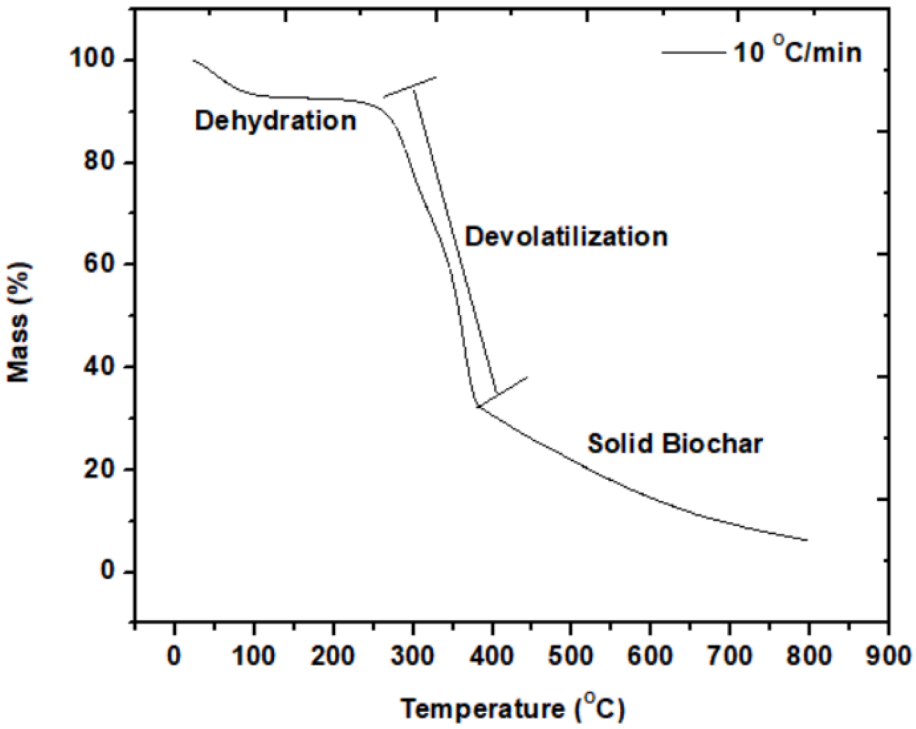

Fig. 3. TGA profile of surface fibers of date palm at 10 °C/min.

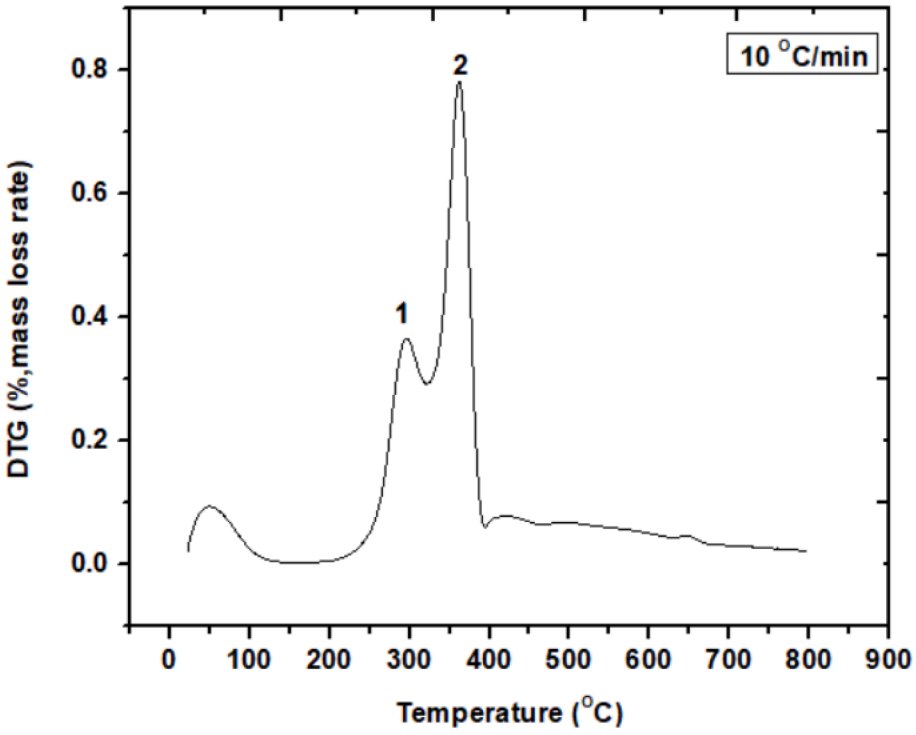

Fig. 4. DTG profile of surface fibers of date palm at 10 °C/min.

their energy density. Biomass materials with higher bulk density are well suited for thermal conversion processes and are easier to handle and transport [50].

Fig. 2 illustrates the FT-IR spectra of surface fibers. Date palm waste materials contain esters, ketones, alkanes, aromatics, and alcohols with different oxygenated functional groups, as it is a lignocellulosic substance composed mainly of cellulose, lignin, and hemicellulose [54]. Because of the presence of C—H and C—O stretching peaks for cellulose linkage, the absorption bands 860 cm^{-1} were formed [55]. The band at 1726 cm^{-1} in the spectra of surface fibers is ascribed to C═O stretching of hemicellulose's uronic ester and acetyl groups or the ester linkage of carboxylic groups of ferulic and p-coumaric acids of lignin or xylan in hemicellulose [56]. The absorption band at 1602 cm^{-1} could be linked to the −C═O stretch of lignin linked p-substituted aryl ketones. [57].

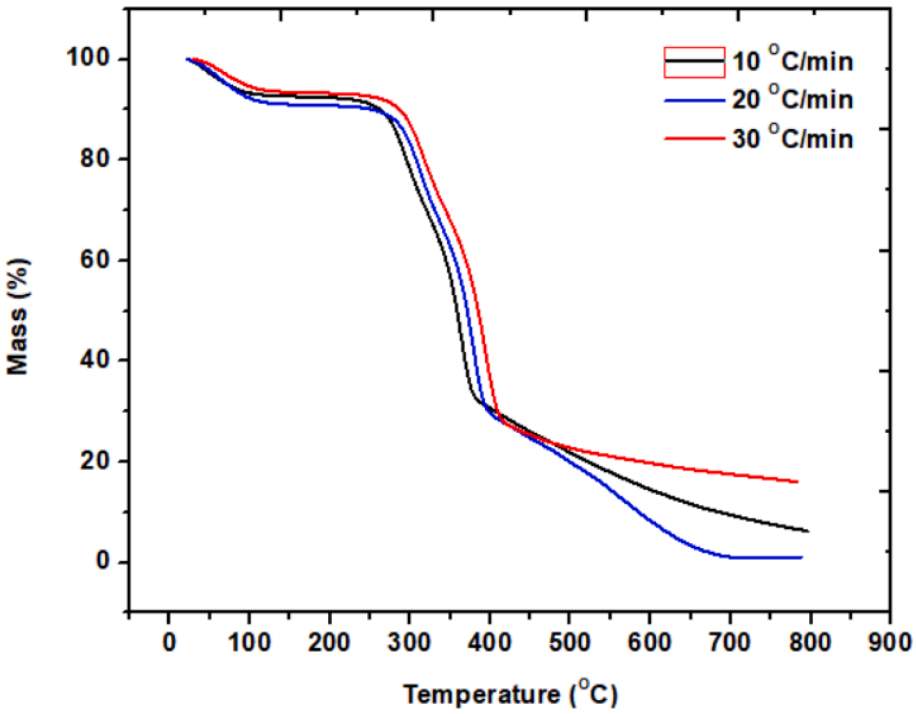

Fig. 5. TGA profiles of surface fibers of date palm at different heating rates (10, 20, and 30 °C/min).

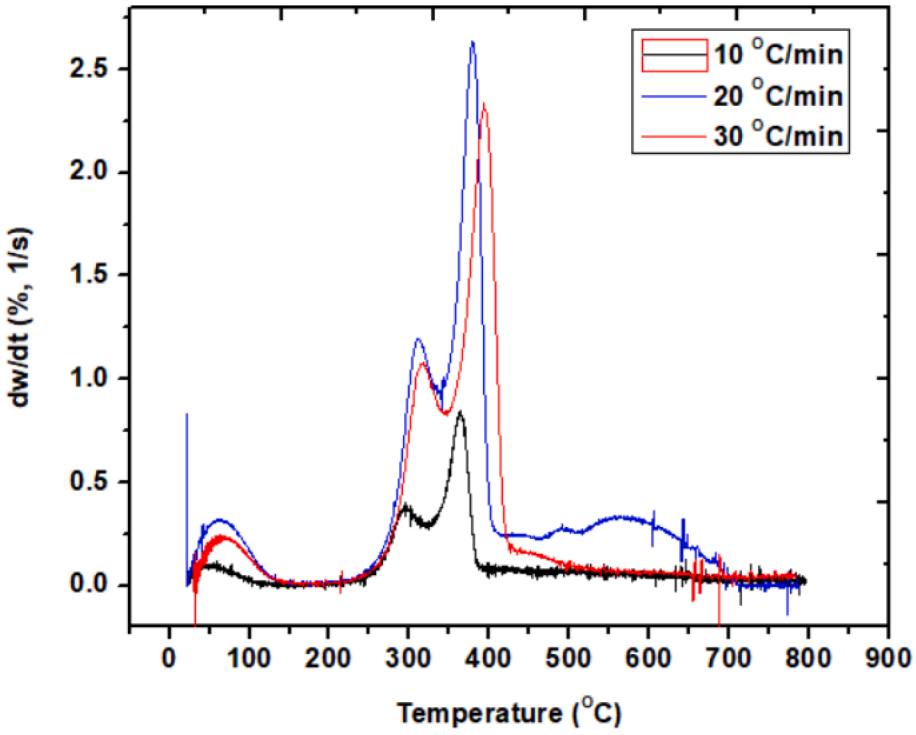

Fig. 6. DTG profiles of surface fibers of date palm at different heating rates (10, 20, and 30 °C/min).

Additional lignin-linked absorption bands include those at 1237 cm^{-1} related to ether C—O—C linkage elongation and 1418 cm^{-1} ascribed to aromatic ring vibrations. [58]. The characteristic peaks that appear for cellulose are at 665 and 1022 cm^{-1} [55]. The expansive absorption band having a peak at 3321 cm^{-1} is owing to the broadening of the −OH groups (hydrogen-bonded) presenting the hydrophilic affinity of the date fibres [59]. At 2919 cm^{-1} is linked to the C—H stretching vibrations [60]. The analysis shows that the functional chemistry is a typical lignocellulosic material consisting of lignin, hemicellulose and cellulose.

3.2. *Thermal decomposition characteristics*

The profile of thermal decomposition of the surface fibers of the date palm is shown in Fig. 3. The profile of thermogravimetric analysis of surface fibers shows that decomposition occurred in three regions:

Table 6
TG-DTG parameters for date palm fibers at multiple heating rates.

Heating rate β (min^{-1})	T_i(°C)	T_f(°C)	T_p(°C)	M_{loss}
10	260	380	360	60 ± 1
20	270	392	378	60 ± 1
30	288	414	395	60 ± 1

T_i = initial temperature of active pyrolysis region.
T_f = final temperature of active pyrolysis region.
T_p = maximum peak temperature/ temperature for maximum decomposition rate.
M_{loss} = percentage mass loss in active pyrolysis region.

dehydration region (20–260 °C), devolatilization region (260–380 °C) and solid combustion stage (380–800 °C). In the dehydration region, there is a 5 percent mass loss due to the removal of unbound moisture up to 100 °C, a 10 percent mass loss due to the removal of bound moisture, and lower hydrocarbons up to 260 °C. The devolatilization region is also described as active pyrolysis. The active pyrolysis region for surface fibers is between 260 and 380 °C. In this region, sixty percent of mass loss takes place. It is known that during the pyrolysis of lignocellulosic materials in the active pyrolysis region, mainly cellulose and hemicellulose, are decomposed. Cellulose and partially hemicellulose generate the volatiles in the active pyrolysis region. Lignin is decomposed after devolatilization, which is described as the passive pyrolysis region [61]. After the devolatilization region, a lignin–rich solid material called biochar remains. In Fig. 4, the DTG curves consist of a moderate peak, a prominent peak, and a long tail representing different reactions during the pyrolysis of surface fibers. The different peaks correspond to the maximum mass loss during the decomposition of hemicellulose, cellulose, and lignin. It is known from the literature that during the pyrolysis of lignocellulosic materials, the first peak corresponds to hemicellulose and the second peak represents the cellulose degradation rate [62]. Hence, it is seen that the maximum volatilities will escape at 360 °C (peak 2, DTG curve) in the active pyrolysis region. Therefore, the evolution of active pyrolysis region components of surface fibers of date palm can be used to infer the formation mechanism of bio-oil and heavy chemicals.

3.3. Effect of heating rate

The TG and DTG curves of date palm fibers pyrolyzed at low and medium heating rates (10 °C, 20, and 30 °C /min) are shown in Fig. 5 and Fig. 6. Similar TG and DTG curve patterns were evident in both ranges of different heating rates. As the heating rates increased, the TG and DTG curves transitioned to higher temperatures, affecting decomposition rates. This is due to the heat and mass transfer delay resulting from a higher heating rate. Table 6 presents data from TG-DTG at 10, 20, and 30 °C /min, along with typical pyrolysis temperatures and percent mass loss. Despite the shift in decomposition temperatures toward higher values, the mass loss/release of volatiles in the active pyrolysis region did not change significantly. The mass loss at all three heating rates (10, 20 and 30 °C /min) in the active pyrolysis region is almost 60 percent. The shape of the DTG curve shows that the active pyrolysis region contains several reactions leading to the degradation of low-temperature thermally stable components (LTSCs). The high-temperature thermally stable components (HTSC) are degraded above 400 °C in the passive pyrolysis region, where the remaining mass loss occurs.

3.4. Kinetic analysis

The estimation of pyrolysis kinetics was carried out in the range of active pyrolysis, which is considered as a one-step mechanism. Based on a study of thermal degradation, several kinetic models with different kinetic mechanisms of pyrolysis could be further recognized after demonstrating the pyrolysis process of date palm fibers. Twenty–one solid-state reaction mechanisms from four reaction mechanism types and the corresponding kinetic parameters (E_a and A) are listed in Table 7. The main solid-state reaction kinetics models can be linearly fitted, and the linear regression coefficient R^2 of each model can be used to determine which model is the best fit. The most appropriate mechanism model would be one with a linear regression coefficient R^2 of 0.99

Table 7
Kinetic parameters of surface fibers of date palm using different solid-state reaction mechanisms.

Model	Heating Rates (°C/min)	E_a(kJ/mol)	R^2	A (min^{-1})
CR0	10	37.58	0.98	0.11
	20	36.77	0.99	0.15
	30	38.39	0.98	0.25
CR1	10	62.42	0.93	42.77
	20	60.27	0.92	39.87
	30	66.09	0.92	144.65
CR1.5	10	129.17	0.69	497.27×10^{6}
	20	124.20	0.55	195.42×10^{6}
	30	147.40	0.53	1.69×10^{10}
CR2	10	103.90	0.76	569.46×10^{3}
	20	100.17	0.63	321.02×10^{3}
	30	116.72	0.61	8.32×10^{6}
CR3	10	158.96	0.59	1.258×10^{11}
	20	149.86	0.50	18.14×10^{9}
	30	180.14	0.49	5.56×10^{12}
DM1	10	84.96	0.99	1.59×10^{3}
	20	83.56	0.99	1.61×10^{3}
	30	87.04	0.99	3.07×10^{3}
DM2	10	19.85	0.62	6.80×10^{-3}
	20	18.46	0.58	8.41×10^{-3}
	30	22.29	0.61	28.12×10^{-3}
DM3	10	38.29	0.92	0.228
	20	36.80	0.90	0.267
	30	40.61	0.90	0.002
DM4	10	97.25	0.99	13.81×10^{3}
	20	95.27	0.99	11.96×10^{3}
	30	100.43	0.99	29.39×10^{3}
DM5	10	102.40	0.98	10.15×10^{3}
	20	100.18	0.98	8.055×10^{3}
	30	106.16	0.98	23.10×10^{3}
DM6	10	158.78	0.88	3.35×10^{9}
	20	153.86	0.84	1.19×10^{9}
	30	119.68	0.97	0.42×10^{6}
DM7	10	114.60	0.97	161.92×10^{3}
	20	111.64	0.97	104.41×10^{3}
	30	119.63	0.97	427.50×10^{3}
DM8	10	102.76	0.98	10.81×10^{3}
	20	100.53	0.98	8.55×10^{3}
	30	106.51	0.98	24.49×10^{3}
GM1	10	48.10	0.98	0.72
	20	46.78	0.97	0.85
	30	49.90	0.98	1.86
GM2	10	52.40	0.97	1.34
	20	50.82	0.96	1.47
	30	54.67	0.97	3.67
NM1	10	13.88	0.97	0.514×10^{-3}
	20	13.39	0.98	8.17×10^{-4}
	30	14.03	0.97	1.28×10^{-3}
NM2	10	5.96	0.94	5.169×10^{-5}
	20	5.57	0.96	8.32×10^{-5}
	30	5.89	0.92	8.32×10^{-5}
NM3	10	2.03	0.77	8.44×10^{-6}
	20	1.69	0.78	1.25×10^{-5}
	30	1.82	0.67	2.01×10^{-5}
NM4	10	26.30	0.90	0.014
	20	25.14	0.89	0.019
	30	27.91	0.89	0.046
NM5	10	14.23	0.87	7.50×10^{-4}
	20	13.40	0.84	1.08×10^{-3}
	30	15.14	0.85	2.28×10^{-3}
NM6	10	38.36	0.92	0.232
	20	36.87	0.90	0.270
	30	40.65	0.90	0.747

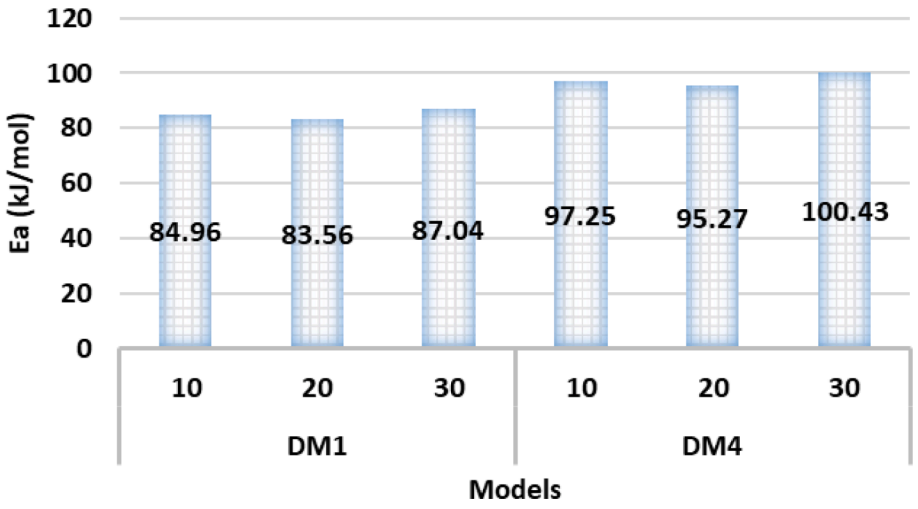

Fig. 7. Average activation energy from two best-fit diffusion models.

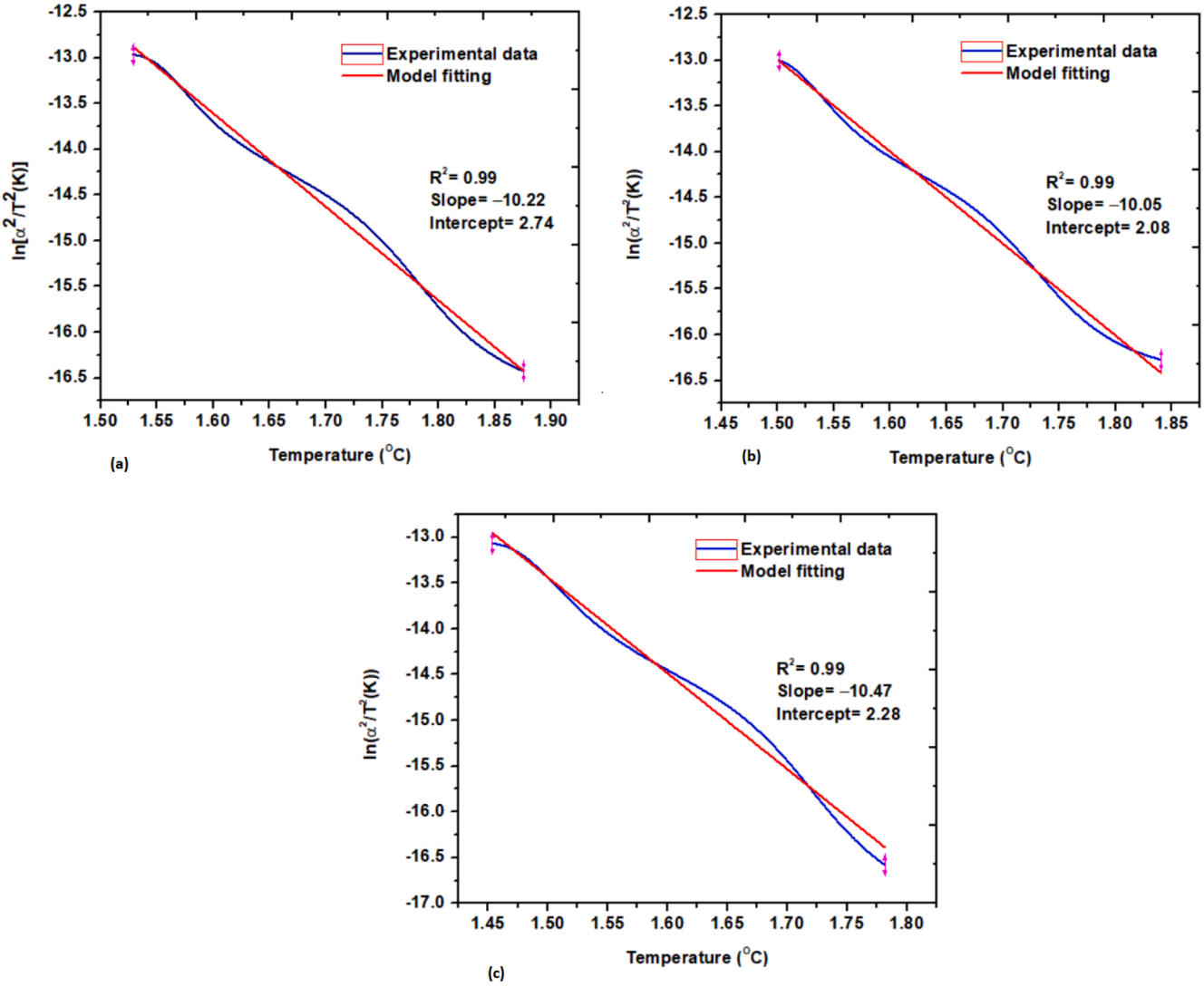

Fig. 8a. Solid-state diffusion model DM1 linear regression with experimental data at a heating rate of (a)- 10 °C/min, (b)- 20 °C/min, and (c)- 30 °C/min.

or equal. The criterion of selecting a suitable model based on the highest regression coefficient (R^2) to estimate the kinetic parameters has already been used by [63] for high ash sewage sludge, [64] for Azadirachta indica and Phyllanthus emblica kernel biomasses, [52] for date seeds, [65] for dry, oily sludge, [66] for paddy husk, [67] for pine and straw pallets, and many others [68]. The Coats-Redfern model-fitting method

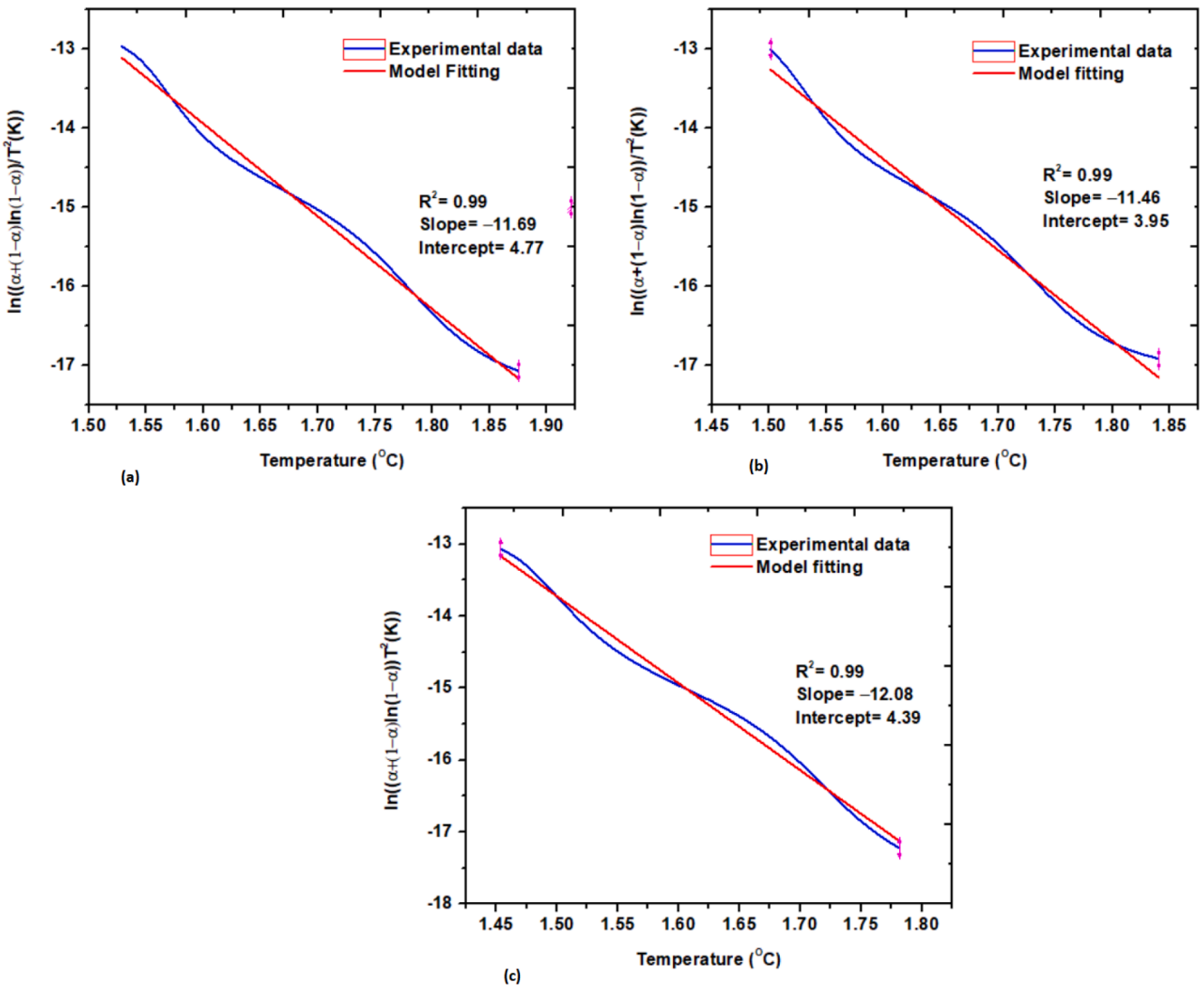

Fig. 8b. Solid-state diffusion model DM4 linear regression with experimental data at a heating rate of (a)- 10 °C/min, (b)- 20 °C/min, and (c)- 30 °C/min.

Table 8
Kinetic parameters of other biomasses evaluated using Coats–Redfern method.

Feedstock	E_a(kJ/mol)	A (min^{-1})	Best–fitted model	Ref.
Date palm surface fibers	84–100	1.59×10^3 –29.39×10^3	Diffusion models (one-way transport & Valensi equation)	This study
Pure glycerol	102.22	8.20×10^9	Chemical reaction–3rd order	[72]
Date leaflets	43.6	1.9×10^5	Chemical reaction–1st order	[52]
Pine and corn starch pellet	218.05	1.28×10^{14}	Diffusion model (spherical symmetry)	[67]
Paddy husk	82	–	Diffusion model (two-dimensional)	[66]
Corn stalk	63–69	10×10^6	Chemical reaction (1st order)	[73]

was utilized to compute the activation energy (E_a) and pre-exponential factor (A, min^{-1}) for the kinetic study of surface fibers of date palm.

Table 7 shows the activation energy, regression coefficient, and pre-exponential factor for different kinetic models in different heating ranges. The pyrolysis temperature range of the devolatilization region for heating rates of 10, 20 and 30 °C /min were 260–380 °C, 270–392 °C and 288–414 °C, respectively. All chemical reaction models (CR1, CR1.5, CR2 and CR3) gave poor regression coefficient values, except CR0. However, the regression coefficient value for CR0 is not consistent at all heating rates. Also, two geometric models (GM1 and GM2) and two nucleation models (NM1 and NM2) had better regression coefficients but were still inconsistent at different heating rates and were below the established criteria for kinetic model selection. All remaining nucleation models (NM3, NM4, NM5, and NM6) had poor regression coefficients. Three diffusion models (DM2, DM3, and DM6) had poor regression coefficient values. Three diffusion models (DM5, DM7, and DM8) had good regression coefficients (R^2 = 0.97–0.98). Diffusion model DM5 has an activation energy of 102.40, 100.18 and 106.16 kJ/mol at a heating rate of 10, 20 and 30 °C /min, respectively. Diffusion model DM7 has activation energy values of 114.60, 111.64 and 119.63 kJ/mol at heating rates of 10, 20, and 30 °C /min, respectively. The DM8 diffusion model has activation energy values of 102.76, 100.53, and 106.51 kJ/mol at heating rates of 10, 20, and 30 °C /min, respectively. Only two diffusion models, the one-way transport (DM1) and the Valensi equation (DM4), showed the best values for the regression coefficient ($R^2 \geq 0.99$) at all three heating rates. The diffusion model DM1 has activation energy values of 84.96, 83.56 and 87.04 kJ/mol at heating rates of 10, 20, and 30 °C /min, respectively, as shown in Fig. 7. Diffusion model DM4 has activation energy values of 97.25, 95.27 and 100.43 kJ/mol at heating rates of 10, 20, and 30 °C /min, respectively, as shown in Fig. 7. Thus,

Table 9
Thermodynamic parameters of surface fibers of date palm pyrolysis.

Model	Heating Rates (°C/min)	ΔH (kJ/mol)	ΔG (kJ/mol)	ΔS (kJ/mol. K)
CR0	10	34.58696	132.9192	−0.27315
	20	33.62731	136.0547	−0.27097
	30	35.10597	140.6068	−0.26709
CR1	10	59.42696	139.9113	−0.22357
	20	57.12731	142.0099	−0.22456
	30	62.80597	147.4184	−0.21421
CR1.5	10	126.177	157.9681	−0.08831
	20	121.0573	157.5266	−0.09648
	30	144.116	167.7234	−0.05977
CR2	10	100.907	152.9676	−0.14461
	20	97.02731	153.6457	−0.14978
	30	113.436	162.0559	−0.12309
CR3	10	155.967	171.1967	−0.0423
	20	146.7173	168.9479	−0.05881
	30	176.856	181.429	−0.01158
DM1	10	81.96696	151.6295	−0.19351
	20	80.41731	153.6771	−0.19381
	30	83.75597	158.3353	−0.18881
DM2	10	16.85696	123.5205	−0.29629
	20	15.31731	126.7995	−0.29493
	30	19.00597	131.6824	−0.28526
DM3	10	35.29696	131.4476	−0.26709
	20	33.65731	134.2726	−0.26618
	30	37.32597	158.6831	−0.30723
DM4	10	94.25696	157.4496	−0.17554
	20	92.12731	159.0849	−0.17714
	30	97.14597	164.3067	−0.17003
DM5	10	99.40696	163.5212	−0.1781
	20	97.03731	165.2371	−0.18042
	30	102.876	170.8276	−0.17203
DM6	10	155.787	181.8687	−0.07245
	20	150.7173	181.5091	−0.08146
	30	116.396	174.8225	−0.14792
DM7	10	111.607	167.4316	−0.15507
	20	108.4973	168.6455	−0.15912
	30	116.346	174.7144	−0.14777
DM8	10	99.76696	163.6927	−0.17757
	20	97.38731	165.3997	−0.17993
	30	103.226	170.9857	−0.17154
GM1	10	45.10696	137.8159	−0.25752
	20	43.63731	140.6134	−0.25655
	30	46.61597	145.5262	−0.25041
GM2	10	49.40696	140.2567	−0.25236
	20	47.67731	142.9319	−0.252
	30	51.38597	148.0643	−0.24476
NM1	10	10.88696	125.2799	−0.31776
	20	10.24731	129.0568	−0.31431
	30	10.74597	133.5688	−0.31094
NM2	10	2.96696	124.2347	−0.33685
	20	2.427308	128.4159	−0.3333
	30	2.60597	134.4052	−0.33367
NM3	10	−0.96304	125.729	−0.35192
	20	−1.45269	130.493	−0.34906
	30	−1.46403	135.0003	−0.34548
NM4	10	23.30696	127.8091	−0.29028
	20	21.99731	130.9182	−0.28815
	30	24.62597	135.6861	−0.28116
NM5	10	11.23696	124.4989	−0.31462
	20	10.25731	128.1898	−0.31199
	30	11.85597	132.7828	−0.30614
NM6	10	35.36696	131.4656	−0.26694
	20	33.72731	134.3075	−0.26609
	30	37.36597	139.2721	−0.25799

based on the best-fit diffusion models (DM1 and DM4), the average activation energy value for date palm fibers is 91.40 kJ/mol. In all reaction mechanism models, including the best-fit diffusion models, when the heating rate is increased from 10 to 20 °C/min, the activation energy drops, but there is an increase in activation energy values when the heating rate is increased from 20 to 30 °C/min. Fig. 8a and Fig. 8b illustrate the liner regression of the best–fit diffusion models (DM1 and DM4) at different heating rates (10, 20, and 30 °C /min).

Table 10
Thermodynamic parameters of other biomasses.

Material	ΔH (kJ/mol)	ΔG (kJ/mol)	ΔS (kJ/mol)	Ref.
Surface fibers (date palm)	80– +97	151– +164	−0.17 to −0.18	This study
Date palm waste	93– +108	205– +280	−0.30 to +0.32	[31]
Date palm leaflets	–	186.5 ± 38.2	0.742 ± 0.13	[32]
Red pepper waste	93.17	105.49	−26.49	[74]
Rice husk	74.28	134.89	−0.18	[33]

For all models of the reaction mechanism, the pre-exponential factor increased with increasing heating rate, as shown in Table 7. The pre-exponential factor represents the frequency of collisions between reaction molecules at a standard concentration. The pre-exponential factor is related to the number of collisions of molecules in the orientation required for a reaction [69]. The best-fitted diffusion models DM1 and DM4 have pre-exponential factor values of the order of thousands (10^3). Diffusion model DM1 has pre-exponential values 1.59×10^3, 1.61×10^3, and 3.07×10^3 min^{-1} at a heating rate of 10, 20, and 30 °C/min. Diffusion model DM4 has pre-exponential values 13.81×10^3, 11.96×10^3, and 29.39×10^3 min^{-1} at a heating rate of 10, 20, and 30 °C/min. Table 8 represents the kinetic parameters of some other biomasses performed using the Coats–Redfern method. Fig. 7 shows an overview of best-fit diffusion models at various heating rates. Gmar Bensidhom et al. [70] performed pyrolysis to obtain bio-oil, biochar, and syngas, from various Tunisian date palm wastes using a fixed-bed reactor at temperatures ranging from room temperature to 500 °C with a heating rate of 15 °C/min. The bio-oil production under these conditions varied from 17.03 to 25.99 wt%. Raza et al. [71] performed pyrolysis of date seeds and coffee waste blend using ASPEN Plus. The effect of pyrolysis operating temperature on pyrolysis products was investigated by changing the temperature in a controlled range from 300 OC to 500 OC. The results show that the production of gases and bio-oil increases linearly with increasing pyrolysis operating temperature up to 450 °C, with gas production increasing and bio-oil production decreasing. Research on the pyrolysis of date waste is progressing. However, pyrolysis kinetic studies help to highlight the potential of waste types and to design the pyrolysis reaction based on kinetic data.

3.5. Thermodynamic parameters

As shown in Table 9, different types of reaction mechanism models were used to determine thermodynamic properties: (1)-change in enthalpy (ΔH), (2) change in Gibbs free energy (ΔG), and (3) change in entropy (ΔS). The thermodynamic parameters were calculated at three different heating rates (10, 20, and 30 °C/min). ΔH values were positive, indicating that the surface fibers of date palm require external energy to start the pyrolysis process. The best-fit diffusion models DM1 and DM2 show an enthalpy change of 80–97 kJ/mol. The change in Gibbs free energy (ΔG) provides informative data about the reaction's spontaneity. All ΔG values of the different models were positive, indicating that pyrolysis of surface fibers of date palm is a non-spontaneous process. The best-fit diffusion models DM1 and DM2 showed a change in Gibbs free energy of 151–164 kJ/mol. The ΔS values were negative, indicating that the disorder of the bond dissociation products was less than that of the original reactants. These negative values indicate that the thermal decay in the activated state has a better-organized structure than before and that the reactions there are more accessible than predicted. The best-fit diffusion models DM1 and DM2 show an entropy change of −0.17003 to −0.18881 kJ/(mol. K). The thermodynamic parameters of the date palm surface fibers are similar to those of other biomasses, as shown in Table 10. The thermodynamic parameters of the investigated date palm fibers are in suitable range in comparison to other

lignocellulosic waste materials. The thermodynamic parameters ΔH and ΔG showed that the pyrolysis of surface fibers is an endothermic and not spontaneous process.

4. Conclusion

The potential of date palm surface fibers has been demonstrated as a valuable feedstock for bio-oil production. The physicochemical properties of the feedstock confirmed the potential for biofuel and bioenergy production. FT-IR and chemical composition analysis confirmed that the surface fibers of date palm are composed of lignocellulose. Thermal degradation of the surface fibers was carried out by thermogravimetric analysis at different heating rates (10, 20 and 30 °C /min) under inert atmosphere and showed that the decomposition is a multistep process with complex behavior. The kinetic analysis of the devolatilization region was performed by the Coats–Redfern model fitting method using twenty-one reaction mechanisms from different solid-state mechanisms. Two diffusion models: one-way transport ($g(x) = \alpha^2$) and Valensi equation ($g(x) = \alpha+(1-\alpha) \times \ln(1-\alpha)$) showed the highest regression coefficient (R^2) with the experimental data. The activation energy (E_a) and the pre-exponential factor (A) was estimated to be 91.40 kJ/mol and 1.59 × 103–29.39 × 10^3 min^{-1}, respectively. The thermodynamic parameters ΔH and ΔG showed that the pyrolysis of surface fibers is an endothermic and not spontaneous process. Since there is no experimental work on the pyrolysis of date palm surface fibers, the reported results are crucial for the design of the pyrolysis process.

CRediT authorship contribution statement

Abrar Inayat: Writing – review & editing. **Farrukh Jamil:** Writing – review & editing. **Shams Forruque Ahmed:** Conceptualization, Investigation. **Muhammad Ayoub:** Supervision, Conceptualization. **Peer Mohamed Abdul:** Investigation. **Muhammad Aslam:** Writing – review & editing. **Md Mofijur:** Supervision, Conceptualization. **Zakir Khan:** Writing – review & editing. **Ahmad Mustafa:** Conceptualization, Investigation.

Declaration of Competing Interest

The authors declare that they have no known competing financial interests or personal relationships that could have appeared to influence the work reported in this paper.

Data availability

No data was used for the research described in the article.

Acknowledgment

The authors would like to acknowledge the financial support from the University of Sharjah, United Arab Emirates, through the Competitive Research Project (21020406177).

References

[1] Ansari KB, Kamal B, Beg S, Khan MAW, Khan MS, Al Mesfer MK, et al. Recent developments in investigating reaction chemistry and transport effects in biomass fast pyrolysis: A review. Renew Sustain Energy Rev 2021;150:111454.
[2] Inayat A, Raza M. District cooling system via renewable energy sources: A review. Renew Sustain Energy Rev 2019;107:360–73.
[3] Santamaria L, Lopez G, Arregi A, Artetxe M, Amutio M, Bilbao J, et al. Catalytic steam reforming of biomass fast pyrolysis volatiles over Ni–Co bimetallic catalysts. J Ind Eng Chem 2020;91:167–81.
[4] Murdock HE, Collier U, Adib R, Hawila D, Bianco E, Muller S, et al. Renewable energy policies in a time of transition. 2018.
[5] Rahman MM, Liu R, Cai J. Catalytic fast pyrolysis of biomass over zeolites for high quality bio-oil–a review. Fuel Process Technol 2018;180:32–46.
[6] Xiu S, Shahbazi A. Bio-oil production and upgrading research: A review. Renew Sustain Energy Rev 2012;16(7):4406–14.
[7] Rocamora I, Wagland ST, Villa R, Simpson EW, Fernández O, Bajón-Fernández Y. Dry anaerobic digestion of organic waste: A review of operational parameters and their impact on process performance. Bioresour Technol 2020;299:122681.
[8] Inayat A, Ahmad MM, Mutalib MIA, Yusup S. Flowsheet development and modeling of hydrogen production from Empty Fruit Bunch via steam gasification. Chem Eng Trans 2010;21:427–32.
[9] Islam MS, Kao N, Bhattacharya SN, Gupta R, Choi HJ. Potential aspect of rice husk biomass in Australia for nanocrystalline cellulose production. Chin J Chem Eng 2018;26(3):465–76.
[10] Inayat A, Jamil F, Raza M, Khurram S, Ghenai C, AaH A-M. Upgradation of waste cooking oil to biodiesel in the presence of green catalyst derived from date seeds. Biofuels 2019:1–6.
[11] Sharifzadeh M, Sadeqzadeh M, Guo M, Borhani TN, Konda NM, Garcia MC, et al. The multi-scale challenges of biomass fast pyrolysis and bio-oil upgrading: Review of the state of art and future research directions. Prog Energy Combust Sci 2019;71:1–80.
[12] Liu R, Sarker M, Rahman MM, Li C, Chai M, Cotillon R, et al. Multi-scale complexities of solid acid catalysts in the catalytic fast pyrolysis of biomass for bio-oil production–A review. Prog Energy Combust Sci 2020;80:100852.
[13] Kumar R, Strezov V, Weldekidan H, He J, Singh S, Kan T, et al. Lignocellulose biomass pyrolysis for bio-oil production: A review of biomass pre-treatment methods for production of drop-in fuels. Renew Sustain Energy Rev 2020;123:109763.
[14] Khan Z, Yusup S, Aslam M, Inayat A, Shahbaz M, Raza Naqvi S, et al. NO and SO2 emissions in palm kernel shell catalytic steam gasification with in-situ CO2 adsorption for hydrogen production in a pilot-scale fluidized bed gasification system. J Clean Prod 2019;236:117636.
[15] Hu X, Gholizadeh M. Progress of the applications of bio-oil. Renew Sustain Energy Rev 2020;134:110124.
[16] Raza M, Inayat A, Ahmed A, Jamil F, Ghenai C, Naqvi SR, et al. Progress of the pyrolyzer reactors and advanced technologies for biomass pyrolysis processing. Sustainability 2021;13(19):11061.
[17] Xie T, Reddy KR, Wang C, Yargicoglu E, Spokas K. Characteristics and applications of biochar for environmental remediation: a review. Crit Rev Environ Sci Technol 2015;45(9):939–69.
[18] Bolan N, Hoang SA, Beiyuan J, Gupta S, Hou D, Karakoti A, et al. Multifunctional applications of biochar beyond carbon storage. Int Mater Rev 2022;67(2):150–200.
[19] Raza M, Inayat A, Khan Z. Designing of a 20 kW updraft fixed-bed biomass gasification power generation system.Advances in Science and Engineering Technology International Conferences (ASET). IEEE 2020;2020:1–6.
[20] Chen X, Chen Y, Yang H, Wang X, Che Q, Chen W, et al. Catalytic fast pyrolysis of biomass: Selective deoxygenation to balance the quality and yield of bio-oil. Bioresour Technol 2019;273:153–8.
[21] Raza M, Abu-Jdayil B. Cellulose nanocrystals from lignocellulosic feedstock: a review of production technology and surface chemistry modification. Cellul 2022:1–38.
[22] Hameed Z, Aman Z, Naqvi SR, Tariq R, Ali I, Makki AA. Kinetic and thermodynamic analyses of sugar cane bagasse and sewage sludge co-pyrolysis process. Energy Fuel 2018;32(9):9551–8.
[23] Hu Z, Zheng Y, Yan F, Xiao B, Liu S. Bio-oil production through pyrolysis of blue-green algae blooms (BGAB): product distribution and bio-oil characterization. Energy 2013;52:119–25.
[24] Çepelioğullar Ö, Pütün AE. Thermal and kinetic behaviors of biomass and plastic wastes in co-pyrolysis. Energ Conver Manage 2013;75:263–70.
[25] Varma RS. Biomass-derived renewable carbonaceous materials for sustainable chemical and environmental applications. ACS Sustain Chem Eng 2019;7(7):6458–70.
[26] Silas K, Ghani WAWAK, Choong TS, Rashid U. Carbonaceous materials modified catalysts for simultaneous SO2/NOx removal from flue gas: A review. Catal Rev 2019;61(1):134–61.
[27] Gamal MS, Asikin-Mijan N, Arumugam M, Rashid U, Taufiq-Yap Y. Solvent-free catalytic deoxygenation of palm fatty acid distillate over cobalt and manganese supported on activated carbon originating from waste coconut shell. J Anal Appl Pyrol 2019;144:104690.
[28] Ahmad J, Rashid U, Patuzzi F, Baratieri M, Taufiq-Yap YH. Synthesis of char-based acidic catalyst for methanolysis of waste cooking oil: An insight into a possible valorization pathway for the solid by-product of gasification. Energ Conver Manage 2018;158:186–92.
[29] Alawar A, Hamed AM, Al-Kaabi K. Characterization of treated date palm tree fiber as composite reinforcement. Compos B Eng 2009;40(7):601–6.
[30] Chaluvadi SR, Khanam S, Aly MA, Bennetzen JL. Genetic diversity and population structure of native and introduced date palm (Phoenix dactylifera) germplasm in the United Arab Emirates. Trop Plant Biol 2014;7(1):30–41.
[31] Raza M, Abu-Jdayil B, Al-Marzouqi AH, Inayat A. Kinetic and thermodynamic analyses of date palm surface fibers pyrolysis using Coats-Redfern method. Renew Energy 2022;183:67–77.
[32] Galiwango E, Al-Marzuoqi AH, Khaleel AA, Abu-Omar MM. Investigation of non-isothermal kinetics and thermodynamic parameters for the pyrolysis of different date palm parts. Energies 2020;13(24):6553.
[33] Naqvi SR, Hameed Z, Tariq R, Taqvi SA, Ali I, Niazi MBK, et al. Synergistic effect on co-pyrolysis of rice husk and sewage sludge by thermal behavior, kinetics, thermodynamic parameters and artificial neural network. Waste Manag 2019;85:131–40.
[34] Raza M, Abdallah HA, Abdullah A, Abu-Jdayil B. Date Palm Surface Fibers for Green Thermal Insulation. Buildings 2022;12(6):866.

[35] Ali I, Tariq R, Naqvi SR, Khoja AH, Mehran MT, Naqvi M, et al. Kinetic and thermodynamic analyses of dried oily sludge pyrolysis. J Energy Inst 2020.
[36] Stefanidis SD, Kalogiannis KG, Iliopoulou EF, Michailof CM, Pilavachi PA, Lappas AA. A study of lignocellulosic biomass pyrolysis via the pyrolysis of cellulose, hemicellulose and lignin. J Anal Appl Pyrol 2014;105:143–50.
[37] Azrina ZZ, Beg MDH, Rosli M, Ramli R, Junadi N, Alam AM. Spherical nanocrystalline cellulose (NCC) from oil palm empty fruit bunch pulp via ultrasound assisted hydrolysis. Carbohydr Polym 2017;162:115–20.
[38] Johar N, Ahmad I, Dufresne A. Extraction, preparation and characterization of cellulose fibres and nanocrystals from rice husk. Ind Crop Prod 2012;37(1):93–9.
[39] Zheng D, Zhang Y, Guo Y, Yue J. Isolation and characterization of nanocellulose with a novel shape from walnut (Juglans regia L.) shell agricultural waste. Polymers 2019;11(7):1130.
[40] Kian L, Saba N, Jawaid M, Alothman O, Fouad H. Properties and characteristics of nanocrystalline cellulose isolated from olive fiber. Carbohydr Polym 2020;241:116423.
[41] Othman I, Pal P, Abu Haija M, Hassan SW, Abu-Jdayil B, AlKhateeb B, et al. Extraction of crystalline nanocellulose from palm tree date seeds (Phoenix dactylifera L.). Chem Eng Commun 2021:1–13.
[42] Beroual M, Trache D, Mehelli O, Boumaza L, Tarchoun AF, Derradji M, et al. Effect of the delignification process on the physicochemical properties and thermal stability of microcrystalline cellulose extracted from date palm fronds. Waste Biomass Valoriz 2021;12(5):2779–93.
[43] Qian C, Li Q, Zhang Z, Wang X, Hu J, Cao W. Prediction of higher heating values of biochar from proximate and ultimate analysis. Fuel 2020;265:116925.
[44] Xing J, Luo K, Wang H, Gao Z, Fan J. A comprehensive study on estimating higher heating value of biomass from proximate and ultimate analysis with machine learning approaches. Energy 2019;188:116077.
[45] Bodude M, Ayoola W, Oyetunji A, Baba Y, Odukoya A, Onifade O, et al. Proximate, ultimate analysis and industrial applications of some Nigerian coals. 2019.
[46] Wang S, Zhao S, Uzoejinwa BB, Zheng A, Wang Q, Huang J, et al. A state-of-the-art review on dual purpose seaweeds utilization for wastewater treatment and crude bio-oil production. Energ Conver Manage 2020;222:113253.
[47] Vassilev SV, Baxter D, Andersen LK, Vassileva CG. An overview of the chemical composition of biomass. Fuel 2010;89(5):913–33.
[48] Shukla N, Sahoo D, Remya N. Biochar from microwave pyrolysis of rice husk for tertiary wastewater treatment and soil nourishment. J Clean Prod 2019;235:1073–9.
[49] Hassan H, Hameed B, Lim J. Co-pyrolysis of sugarcane bagasse and waste high-density polyethylene: Synergistic effect and product distributions. Energy 2020;191:116545.
[50] Bhagwanrao SV, Singaravelu M. Bulk density of biomass and particle density of their briquettes. International Journal of Agricultural Engineering 2014;7(1):221–4.
[51] Babiker ME, Aziz ARA, Heikal M, Yusup S. Pyrolysis characteristics of Phoenix dactylifera date palm seeds using thermo-gravimetric analysis (TGA). International Journal of Environmental Science and Development 2013;4(5):521.
[52] Sait HH, Hussain A, Salema AA, Ani FN. Pyrolysis and combustion kinetics of date palm biomass using thermogravimetric analysis. Bioresour Technol 2012;118:382–9.
[53] Kaliyan N, Morey RV, White MD, Tiffany DG. A tub-grinding/roll-press compaction system to increase biomass bulk density: preliminary study. *2009 Reno, Nevada, June 21-June 24, 2009*. American Society of Agricultural and Biological Engineers; 2009:1.
[54] Lamaming J, Hashim R, Leh CP, Sulaiman O, Sugimoto T, Nasir M. Isolation and characterization of cellulose nanocrystals from parenchyma and vascular bundle of oil palm trunk (Elaeis guineensis). Carbohydr Polym 2015;134:534–40.
[55] Adel AM, Abd El-Wahab ZH, Ibrahim AA, Al-Shemy MT. Characterization of microcrystalline cellulose prepared from lignocellulosic materials. Part II: Physicochemical properties. Carbohydrate Polym 2011;83(2):676–87.
[56] Kalita E, Nath B, Agan F, More V, Deb P. Isolation and characterization of crystalline, autofluorescent, cellulose nanocrystals from saw dust wastes. Ind Crop Prod 2015;65:550–5.
[57] Himmelsbach DS, Khalili S, Akin DE. The use of FT-IR microspectroscopic mapping to study the effects of enzymatic retting of flax (Linum usitatissimum L) stems. J Sci Food Agric 2002;82(7):685–96.
[58] Bykov I. Characterization of natural and technical lignins using FTIR spectroscopy (http://www.diva-portal.org/smash/get/diva2:1016107/FULLTEXT01.pdf). thesis 2008.
[59] Wang Z, Yao Z, Zhou J, He M, Jiang Q, Li S, et al. Isolation and characterization of cellulose nanocrystals from pueraria root residue. Int J Biol Macromol 2019;129:1081–9.
[60] Oun AA, Rhim J-W. Preparation and characterization of sodium carboxymethyl cellulose/cotton linter cellulose nanofibril composite films. Carbohydr Polym 2015;127:101–9.
[61] Zhong D, Zeng K, Li J, Qiu Y, Flamant G, Nzihou A, et al. Characteristics and evolution of heavy components in bio-oil from the pyrolysis of cellulose, hemicellulose and lignin. Renew Sustain Energy Rev 2022;157:111989.
[62] White JE, Catallo WJ, Legendre BL. Biomass pyrolysis kinetics: a comparative critical review with relevant agricultural residue case studies. J Anal Appl Pyrol 2011;91(1):1–33.
[63] Naqvi SR, Tariq R, Hameed Z, Ali I, Naqvi M, Chen W-H, et al. Pyrolysis of high ash sewage sludge: Kinetics and thermodynamic analysis using Coats-Redfern method. Renew Energy 2019;131:854–60.
[64] Mishra RK, Mohanty K. Kinetic analysis and pyrolysis behaviour of waste biomass towards its bioenergy potential. Bioresour Technol 2020;311:123480.
[65] Ali I, Tariq R, Naqvi SR, Khoja AH, Mehran MT, Naqvi M, et al. Kinetic and thermodynamic analyses of dried oily sludge pyrolysis. J Energy Inst 2021;95:30–40.
[66] Naqvi SR, Uemura Y, Osman N, Yusup S. Kinetic study of the catalytic pyrolysis of paddy husk by use of thermogravimetric data and the Coats-Redfern model. Res Chem Intermed 2015;41(12):9743–55.
[67] Mian I, Li X, Jian Y, Dacres OD, Zhong M, Liu J, et al. Kinetic study of biomass pellet pyrolysis by using distributed activation energy model and Coats Redfern methods and their comparison. Bioresour Technol 2019;294:122099.
[68] Hameed S, Sharma A, Pareek V, Wu H, Yu Y. A review on biomass pyrolysis models: Kinetic, network and mechanistic models. Biomass Bioenergy 2019;123:104–22.
[69] Balasundram V, Ibrahim N, Kasmani RM, Hamid MKA, Isha R, Hasbullah H, et al. Thermogravimetric catalytic pyrolysis and kinetic studies of coconut copra and rice husk for possible maximum production of pyrolysis oil. J Clean Prod 2017;167:218–28.
[70] Bensidhom G, Hassen-Trabelsi AB, Alper K, Sghairoun M, Zaafouri K, Trabelsi I. Pyrolysis of Date palm waste in a fixed-bed reactor: Characterization of pyrolytic products. Bioresour Technol 2018;247:363–9.
[71] Raza M, Inayat A, Al Jaberi B, Said Z, Ghenai C. Simulation of the pyrolysis process using blend of date seeds and coffee waste as biomass. *2020 Advances in Science and Engineering Technology International Conferences (ASET)*. IEEE; 2020:1-5.
[72] Almazrouei M, Janajreh I. Model-fitting approach to kinetic analysis of non-isothermal pyrolysis of pure and crude glycerol. Renew Energy 2020;145:1693–708.
[73] Zhang X, Xu M, Sun R, Sun L. Study on biomass pyrolysis kinetics. 2006.
[74] Maia AAD, de Morais LC. Kinetic parameters of red pepper waste as biomass to solid biofuel. Bioresour Technol 2016;204:157–63.